

Double Spin Asymmetries of Inclusive Hadron Electroproductions from a Transversely Polarized ^3He Target

Y.X. Zhao,^{1,*} K. Allada,^{2,3} K. Aniol,⁴ J.R.M. Annand,⁵ T. Averett,⁶ F. Benmokhtar,⁷ W. Bertozzi,² P.C. Bradshaw,⁶ P. Bosted,³ A. Camsonne,³ M. Canan,⁸ G.D. Cates,⁹ C. Chen,¹⁰ J.-P. Chen,³ W. Chen,¹¹ K. Chirapatpimol,⁹ E. Chudakov,³ E. Cisbani,^{12,13} J.C. Cornejo,⁴ F. Cusanno,^{14,†} M. Dalton,⁹ W. Deconinck,² C.W. de Jager,^{3,9} R. De Leo,¹⁵ X. Deng,⁹ A. Deur,³ H. Ding,⁹ P. A. M. Dolph,⁹ C. Dutta,¹⁶ D. Dutta,¹⁷ L. El Fassi,¹⁸ S. Frullani,^{14,13} H. Gao,¹¹ F. Garibaldi,^{14,13} D. Gaskell,³ S. Gilad,² R. Gilman,^{3,18} O. Glamazdin,¹⁹ S. Golge,⁸ L. Guo,^{20,21} D. Hamilton,⁵ O. Hansen,³ D.W. Higinbotham,³ T. Holmstrom,²² J. Huang,^{2,20} M. Huang,¹¹ H. F Ibrahim,²³ M. Iodice,²⁴ X. Jiang,^{18,20} G. Jin,⁹ M.K. Jones,³ J. Katich,⁶ A. Kelleher,⁶ W. Kim,²⁵ A. Kolarkar,¹⁶ W. Korsch,¹⁶ J.J. LeRose,³ X. Li,²⁶ Y. Li,²⁶ R. Lindgren,⁹ N. Liyanage,⁹ E. Long,²⁷ H.-J. Lu,¹ D.J. Margaziotis,⁴ P. Markowitz,²¹ S. Marrone,¹⁵ D. McNulty,²⁸ Z.-E. Meziani,²⁹ R. Michaels,³ B. Moffit,^{2,3} C. Muñoz Camacho,³⁰ S. Nanda,³ A. Narayan,¹⁷ V. Nelyubin,⁹ B. Norum,⁹ Y. Oh,³¹ M. Osipenko,³² D. Parno,⁷ J.-C. Peng,³³ S. K. Phillips,³⁴ M. Posik,²⁹ A. J. R. Puckett,^{2,20} X. Qian,³⁵ Y. Qiang,^{11,3} A. Rakhman,³⁶ R. Ransome,¹⁸ S. Riordan,⁹ A. Saha,^{3,†} B. Sawatzky,^{29,3} E. Schulte,¹⁸ A. Shahinyan,³⁷ M. H. Shabestari,⁹ S. Širca,³⁸ S. Stepanyan,³⁹ R. Subedi,⁹ V. Sulkosy,^{2,3} L.-G. Tang,¹⁰ W. A. Tobias,⁹ G. M. Urciuoli,¹⁴ I. Vilardi,¹⁵ K. Wang,⁹ B. Wojtsekhowski,³ Y. Wang,³³ X. Yan,¹ H. Yao,²⁹ Y. Ye,¹ Z. Ye,¹⁰ L. Yuan,¹⁰ X. Zhan,² Y. Zhang,⁴⁰ Y.-W. Zhang,⁴⁰ B. Zhao,⁶ X. Zheng,⁹ L. Zhu,^{33,10} X. Zhu,¹¹ and X. Zong¹¹

(The Jefferson Lab Hall A Collaboration)

¹University of Science and Technology of China, Hefei 230026, People's Republic of China

²Massachusetts Institute of Technology, Cambridge, MA 02139

³Thomas Jefferson National Accelerator Facility, Newport News, VA 23606

⁴California State University, Los Angeles, Los Angeles, CA 90032

⁵University of Glasgow, Glasgow G12 8QQ, Scotland, United Kingdom

⁶College of William and Mary, Williamsburg, VA 23187

⁷Carnegie Mellon University, Pittsburgh, PA 15213

⁸Old Dominion University, Norfolk, VA 23529

⁹University of Virginia, Charlottesville, VA 22904

¹⁰Hampton University, Hampton, VA 23187

¹¹Duke University, Durham, NC 27708

¹²INFN, Sezione di Roma, I-00185 Rome, Italy

¹³Istituto Superiore di Sanità, I-00161 Rome, Italy

¹⁴INFN, Sezione di Roma, I-00161 Rome, Italy

¹⁵INFN, Sezione di Bari and University of Bari, I-70126 Bari, Italy

¹⁶University of Kentucky, Lexington, KY 40506

¹⁷Mississippi State University, MS 39762

¹⁸Rutgers, The State University of New Jersey, Piscataway, NJ 08855

¹⁹Kharkov Institute of Physics and Technology, Kharkov 61108, Ukraine

²⁰Los Alamos National Laboratory, Los Alamos, NM 87545

²¹Florida International University, Miami, FL 33199

²²Longwood University, Farmville, VA 23909

²³Cairo University, Giza 12613, Egypt

²⁴INFN, Sezione di Roma Tre, I-00146 Rome, Italy

²⁵Kyungpook National University, Taegu 702-701, Republic of Korea

²⁶China Institute of Atomic Energy, Beijing, People's Republic of China

²⁷Kent State University, Kent, OH 44242

²⁸University of Massachusetts, Amherst, MA 01003

²⁹Temple University, Philadelphia, PA 19122

³⁰Université Blaise Pascal/IN2P3, F-63177 Aubière, France

³¹Seoul National University, Seoul, South Korea

³²INFN, Sezione di Genova, I-16146 Genova, Italy

³³University of Illinois, Urbana-Champaign, IL 61801

³⁴University of New Hampshire, Durham, NH 03824

³⁵Physics Department, Brookhaven National Laboratory, Upton, NY

³⁶Syracuse University, Syracuse, NY 13244

³⁷Yerevan Physics Institute, Yerevan 375036, Armenia

³⁸University of Ljubljana, SI-1000 Ljubljana, Slovenia

³⁹Kyungpook National University, Taegu City, South Korea

⁴⁰Lanzhou University, Lanzhou 730000, Gansu, People's Republic of China

We report the measurement of beam-target double-spin asymmetries (A_{LT}) in the inclusive production of identified hadrons, $\bar{e} + {}^3\text{He}^\uparrow \rightarrow h + X$, using a longitudinally polarized 5.9 GeV electron beam and a transversely polarized ${}^3\text{He}$ target. Hadrons (π^\pm , K^\pm and proton) were detected at 16° with an average momentum $\langle P_h \rangle = 2.35$ GeV/c and a transverse momentum (p_T) coverage from 0.60 to 0.68 GeV/c. Asymmetries from the ${}^3\text{He}$ target were observed to be non-zero for π^\pm production when the target was polarized transversely in the horizontal plane. The π^+ and π^- asymmetries have opposite signs, analogous to the behavior of A_{LT} in semi-inclusive deep-inelastic scattering.

PACS numbers: 14.20.Dh, 25.30.Fj, 25.30.Rw, 24.85.+p

I. INTRODUCTION

Understanding the spin structure of the nucleon remains an important goal of research in modern hadronic physics. Beam-target double-spin asymmetries (DSA) have been used as a powerful tool in polarized lepton-nucleon deep-inelastic scattering (DIS) experiments to extract polarized parton distributions and quark-gluon correlations [1]. Earlier efforts have been focused mainly on the longitudinal spin structure g_1 . Recently, with transversely polarized nucleons, DSAs were used to investigate the g_2 structure functions, which involve twist-3 effects. More recently, a measurement of DSA with a transversely polarized nucleon (A_{LT}) in a semi-inclusive deep-inelastic scattering (SIDIS) experiment has provided access to the transverse-momentum-dependent parton distribution functions $g_{1T}(x, k_t^2)$, which are related to quark spin-orbit correlations [2]. In this paper, a measurement of A_{LT} in a less explored reaction, $\bar{e} + N^\uparrow \rightarrow h + X$, in which a single hadron is detected in the final state, is presented.

The mechanism of inclusive hadron photoproduction was studied in [3, 4]. The production of hadrons arises mainly from four types of processes: fragmentation processes, direct processes, resolved photon processes and soft contributions. Fragmentation processes have quarks and gluons produced in short-range reactions followed by fragmentation at long distances of either a quark or a gluon to produce the observed hadron. Direct processes occur when the hadron is produced in a short-range reaction via a radiated gluon giving a quark-antiquark pair, one of which joins the initial quark to produce the hadron. Resolved processes are contributions in which photons fluctuate into a quark-antiquark pair, which then interact with the partons of the target. Soft contributions are described by the vector meson dominance (VMD) approximation, which is a way to represent the hadronic components of the photon as they enter into soft processes.

In the collinear factorization framework, A_{LT} in inclusive hadron production is an observable associated with twist-3 effects. It can have twist-3 contributions from both the parton distributions inside the polarized nucleon

and the parton fragmentation into final state hadrons. By measuring A_{LT} , one has the opportunity to investigate the “worm-gear”-type function $\tilde{g}(x)$ [5, 6] as well as the role of quark-gluon-quark correlations in the nucleon and twist-3 effects in the fragmenting hadron. The $\tilde{g}(x)$ is defined as an integration [5] over k_t^2 of $g_{1T}(x, k_t^2)$, which can be accessed by A_{LT} measurements in a SIDIS process [2]. Furthermore, it has been proposed that $\tilde{g}(x)$ and quark-gluon-quark correlations are responsible for DSAs of inclusive jet (or hadron) production in polarized nucleon-nucleon reactions and lepton-nucleon reactions in [7, 8].

In this paper, we report a measurement of beam-target double-spin asymmetries in inclusive charged-hadron production using a longitudinally polarized electron beam scattered from a transversely polarized ${}^3\text{He}$ target. The measured asymmetry is defined as

$$A_{LT} = \frac{1}{|P_B P_{target}|} \frac{d\sigma^{\uparrow\rightarrow} - d\sigma^{\downarrow\rightarrow}}{d\sigma^{\uparrow\rightarrow} + d\sigma^{\downarrow\rightarrow}}, \quad (1)$$

where $d\sigma^{\uparrow(\downarrow)\rightarrow}$ is the differential cross-section for beam helicity + (-) in a certain target spin direction. P_B is the beam polarization and P_{target} is the target polarization. Figure 1 shows the kinematical configuration in the laboratory coordinate system of the measurement. ϕ_s is the azimuthal angle between the target spin direction \vec{S} and the “hadron plane” which is formed by the incoming electron and the outgoing hadron. The spin-dependent part of the cross-section is proportional to the term $\lambda_e \vec{S} \cdot \vec{p}_T$ ($p_T = \sqrt{p_x^2 + p_y^2}$, the transverse momentum of the outgoing hadron), which gives rise to a $\cos(\phi_s)$ modulation in the definition of the asymmetry [5]. In order to form the parity-even structure by using the spin of the nucleon and the momentum of outgoing hadron, $\cos(\phi_s)$ is the only modulation considered in the current theoretical framework [5]. Hence, the asymmetry can be written as

$$A_{LT} = A_{LT}^{\cos(\phi_s)} \cos(\phi_s). \quad (2)$$

The produced hadrons were detected in a high-resolution spectrometer (HRS) [9] at a central angle of 16° on the beam left side with a central momentum of 2.35 GeV/c, a momentum acceptance of $\pm 4.5\%$ and solid angle acceptance of 6 msr. The data were collected using a singles trigger during the E06-010 experiment [2, 10–12] in Hall A at Jefferson Lab.

* Corresponding author: yxzhao@jlab.org

† Deceased

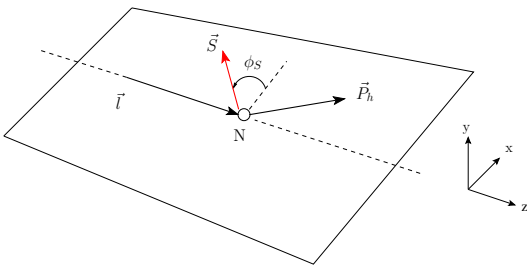


FIG. 1. (Color online) Kinematical configuration in the laboratory coordinate system for the $\bar{e}N^{\uparrow} \rightarrow hX$ process. \vec{l} (\vec{P}_h) represents the momentum direction of the incident electron (produced hadron), and \vec{S} is the spin vector of the nucleon. During the experiment, the target spin was oriented in $\phi_s = 0^\circ(+x), 90^\circ(+y), 180^\circ(-x), 270^\circ(-y)$ directions.

II. EXPERIMENT

A polarized 5.9 GeV electron beam with an average current of 12 μA was provided by the CEBAF accelerator during the experiment. Polarized electrons were excited from a strained superlattice GaAs photocathode by a circularly polarized laser [13] at the injector. The average beam polarization was $(76.8 \pm 3.5)\%$, which was measured periodically by Møller polarimeter [9]. The beam helicity was reversed at 30 Hz by flipping the laser polarization. During the E06-010 experiment, the sequence for beam helicity states followed a quartet structure, $+-$ or $-++-$, randomly to reduce the systematic bias between the two helicity states. Due to a beam-charge feedback system [14], the beam-charge asymmetry between the two helicity states was kept at less than 150 ppm per 20 minutes and less than 10 ppm for the entire experiment [2].

The ground state of the ^3He nuclear wavefunction is dominated by the S-state, in which the proton spins cancel each other and the nuclear spin is carried by the neutron [15]. About 10 atm of ^3He gas was filled in a 40 cm-long cylindrical aluminosilicate glass cell and ^3He nuclei were polarized by spin-exchange optical pumping of a Rb-K mixture [16, 17]. Three pairs of Helmholtz coils were used in the experiment to orient the magnetic holding field transversely or vertically with respect to the electron beam. For each orientation, the spin direction of ^3He nuclei was flipped every 20 minutes through adiabatic fast passage. Nuclear magnetic resonance measurements, calibrated by the electron paramagnetic resonance method [18], were performed to monitor the target polarization while the target spin direction was flipped. An average in-beam target polarization of $(55.4 \pm 2.8)\%$ was achieved during the experiment.

The HRS detector package was configured for hadron detection. The trigger was formed by the coincidence signal between two scintillator planes which were about 2 meters apart. Four detectors were used for particle identification: 1) a threshold CO_2 gas Cerenkov detector for electron identification, 2) a threshold aerogel

Cerenkov detector for pion identification, 3) a ring imaging Cerenkov (RICH) detector for π^\pm , K^\pm , and proton identification [11, 19], 4) two layers of lead-glass calorimeter for electron-hadron separation. Contaminations were well controlled and studied carefully in [11].

III. DATA ANALYSIS

For each target spin direction, the selected data samples were separated into two groups by beam helicity states. These two groups were treated as a “local pair”. The final beam-target double-spin asymmetry A_{LT} was extracted by summing over all “local pair” measurements.

A small amount of N_2 gas, present in the target cell to reduce depolarization [9], diluted the measured ^3He asymmetry and was corrected by the nitrogen dilution factor defined as

$$f_{\text{N}_2} = \frac{\rho_{\text{N}_2} \sigma_{\text{N}_2}}{\rho_{^3\text{He}} \sigma_{^3\text{He}} + \rho_{\text{N}_2} \sigma_{\text{N}_2}}, \quad (3)$$

where ρ is the density of the gas in the production target cell and σ is the unpolarized inclusive hadron (pion, kaon and proton) production cross section. The ratio of unpolarized cross sections $\sigma_{\text{N}_2}/\sigma_{^3\text{He}}$ was measured in dedicated runs on targets filled with known amounts of unpolarized N_2 or ^3He gas. The f_{N_2} in this experiment was determined to be less than 10%.

The overall systematic uncertainty in the experiment was small due to frequent target-spin and beam-helicity flips. The false asymmetry due to luminosity fluctuations was less than 0.07% and was confirmed by measuring the beam-target double-spin asymmetry in the inclusive (e,e') DIS reaction with the target polarized in the $\pm y$ direction, in which the asymmetry vanishes due to parity and time-reversal symmetry. Systematic uncertainties due to contaminations were estimated to be less than 0.02% for pion, kaon and proton measurements. In addition, there was an overall 5% systematic uncertainty, relative to the asymmetries, from both beam and target polarizations. For the kaon and proton measurements, as described in [11], there were two additional sources of systematic uncertainties associated with the RICH detector: 1) the value of the cut on the number of hits in the RICH detector; 2) detector inefficiencies. The first contribution was determined to be $<15\%$ for K^\pm , and $<3\%$ for protons, relative to the statistical uncertainties. The second contribution was determined to be $<7\%$, $<3\%$, and $<1\%$, relative to the statistical uncertainties, for K^+ , K^- and protons, respectively.

IV. RESULTS

The final A_{LT} results from ^3He are shown for different hadron species in Figure 2 and tabulated in Table III. The

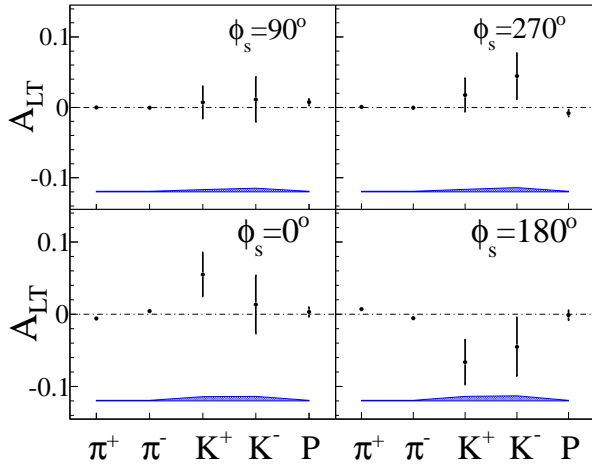


FIG. 2. (Color online) Beam-target double-spin asymmetries A_{LT} for π^\pm , K^\pm and proton production from ${}^3\text{He}$ for different ϕ_s .

$\langle p_T \rangle$ (GeV/c)	π^+ ($A_{LT}^{\cos(\phi_s)} \pm \text{Stat.} \pm \text{Sys.}$)	π^- ($A_{LT}^{\cos(\phi_s)} \pm \text{Stat.} \pm \text{Sys.}$)
0.60	$-0.0081 \pm 0.0018 \pm 0.0009$	$0.0054 \pm 0.0012 \pm 0.0008$
0.64	$-0.0067 \pm 0.0022 \pm 0.0008$	$0.0048 \pm 0.0014 \pm 0.0008$
0.68	$-0.0043 \pm 0.0020 \pm 0.0008$	$0.0046 \pm 0.0013 \pm 0.0008$

TABLE I. Tabulated results of p_T dependent $A_{LT}^{\cos(\phi_s)}$ for π^\pm production from ${}^3\text{He}$.

error bars represent the statistical uncertainties. Experimental systematic uncertainties, combined in quadrature from different sources, are shown as a band. For $\phi_s = 90^\circ$ and 270° , the asymmetries from pions and kaons are consistent with zero within the experimental uncertainties ($\sim 1 \times 10^{-3}$ level for the pion measurement). For $\phi_s = 0^\circ$ and 180° , the sign of the asymmetry is flipped when the target spin direction is reversed. Pion data were also analyzed in three p_T bins. The results are shown in Figure 3. The asymmetries for $\phi_s = 0^\circ$ and $\phi_s = 180^\circ$ were combined together to obtain $A_{LT}^{\cos(\phi_s)}$. The combination was weighted by the statistical uncertainties of the asymmetries. The final p_T -dependent $A_{LT}^{\cos(\phi_s)}$ asymmetries for π^\pm production from ${}^3\text{He}$ are shown in Figure 4 and tabulated in Table I.

Neutron asymmetries for pion production were obtained from the ${}^3\text{He}$ asymmetries using the effective polarizations of the proton and neutron in polarized ${}^3\text{He}$ using the equation [20],

$$A_{LT}^{3\text{He}} = P_n(1 - f_p)A_{LT}^n + P_p f_p A_{LT}^p, \quad (4)$$

where $A_{LT}^{3\text{He}}$ is the measured ${}^3\text{He}$ asymmetry. $P_n = 0.86^{+0.036}_{-0.02}$ and $P_p = -0.028^{+0.009}_{-0.004}$ are the effective polarization of the neutron and proton in polarized ${}^3\text{He}$ respectively. The proton dilutions, $f_p = \frac{2\sigma_p}{\sigma_{3\text{He}}}$, in ${}^3\text{He}$ were measured directly

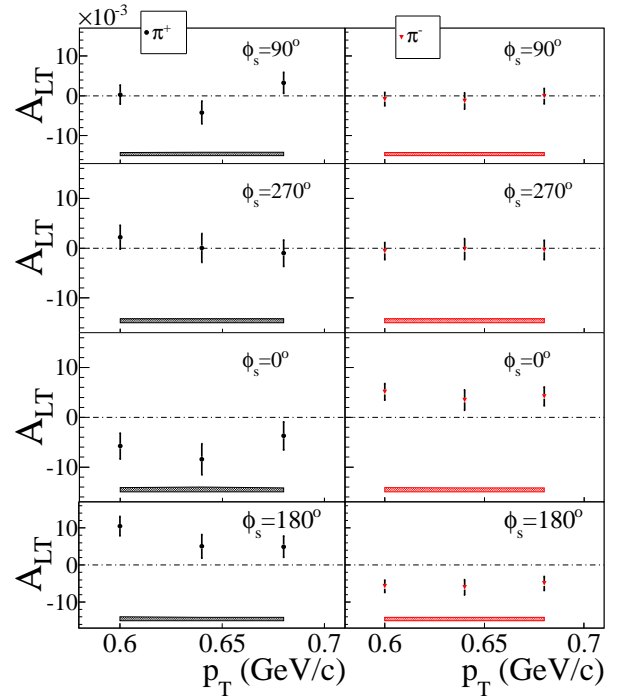


FIG. 3. (Color online) Beam-target double-spin asymmetries A_{LT} for π^\pm production from ${}^3\text{He}$ as a function of p_T for different ϕ_s . The left column is for the π^+ data, the right column is for the π^- data.

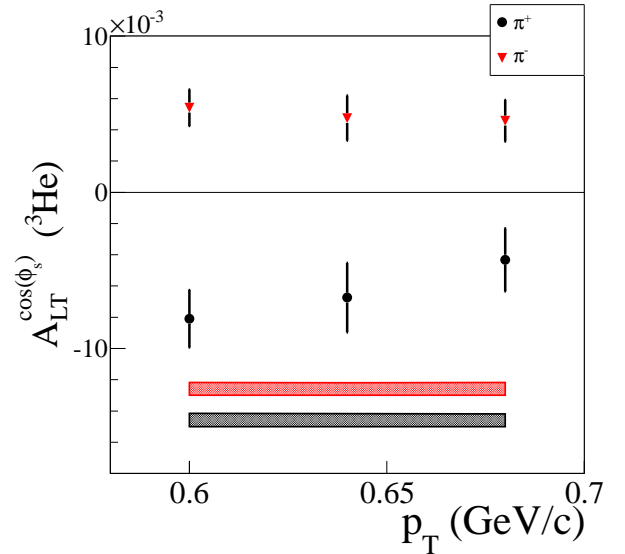


FIG. 4. (Color online) Beam-target double-spin asymmetries $A_{LT}^{\cos(\phi_s)}$ for π^\pm production from ${}^3\text{He}$ as a function of p_T . The red (top) band is the systematic uncertainty band for π^- , and the black (bottom) band is the systematic uncertainty band for π^+ .

$\langle p_T \rangle$ (GeV/c)	$\langle x_F \rangle$	π^+ ($A_{LT}^{\cos(\phi_s)} \pm \text{Stat.} \pm \text{Sys.}$)	π^- ($A_{LT}^{\cos(\phi_s)} \pm \text{Stat.} \pm \text{Sys.}$)
0.60	-0.269	$-0.063 \pm 0.014 \pm 0.012$	$0.024 \pm 0.005 \pm 0.006$
0.64	-0.263	$-0.049 \pm 0.016 \pm 0.011$	$0.020 \pm 0.006 \pm 0.006$
0.68	-0.254	$-0.032 \pm 0.015 \pm 0.011$	$0.019 \pm 0.005 \pm 0.005$

TABLE II. Tabulated results of p_T dependent $A_{LT}^{\cos(\phi_s)}$ for π^\pm production from the neutron. A negative x_F indicates that the produced hadron is moving backwards with respect to the nucleon momentum direction in the center-of-mass frame of the e+N system.

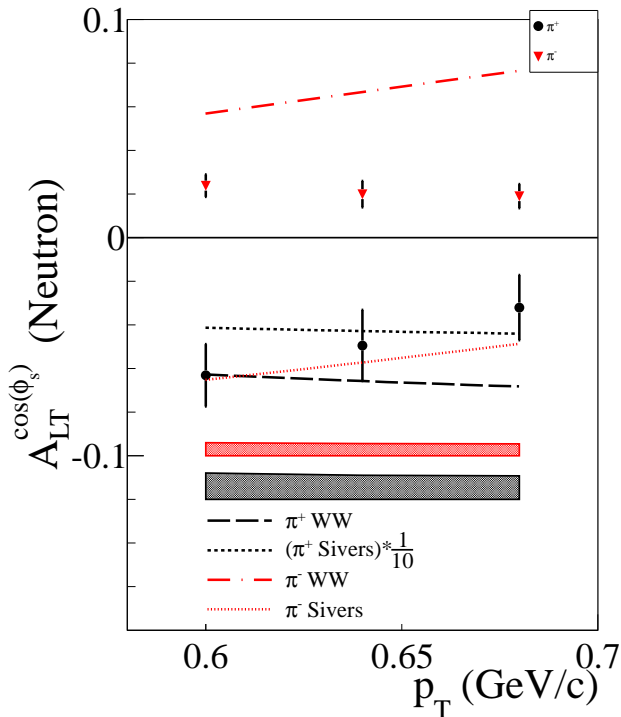


FIG. 5. (Color online) Beam-target double-spin asymmetries $A_{LT}^{\cos(\phi_s)}$ for π^\pm production from the neutron as a function of p_T . The systematic uncertainty is shown as a band. The red (top) band is the systematic uncertainty band for π^- , and the black (bottom) band is the systematic uncertainty band for π^+ . Predictions from collinear factorization by using two different scenarios [5] (Sivers function and Wandzura-Wilczek(WW)-type approximation) are shown as well. Please note that the prediction for π^+ by using the Sivers function is scaled by a factor of $\frac{1}{10}$.

by measuring yields from unpolarized hydrogen and ^3He targets. The average of f_p for π^+ was 0.844 ± 0.007 and for π^- , 0.732 ± 0.005 . Since there were no A_{LT} experimental data from the proton, and the contribution to the final ^3He asymmetry from polarized protons in polarized ^3He is small due to the small P_p , the proton A_{LT}^p was treated as a systematic uncertainty while the neutron asymmetry was extracted from the ^3He asymmetry. The beam-target double-spin asymmetry from a polarized proton target was assumed to be no more than $\pm 5\%$ based on the calculations for a proton target in [5]. The

final p_T -dependent asymmetries $A_{LT}^{\cos(\phi_s)}$ for π^\pm production from the neutron are shown in Figure 5 and tabulated in Table II. In addition, the kinematic variable x_F was also calculated. It is defined as $x_F = 2p^{CM}/\sqrt{s}$, where p^{CM} is the momentum of the outgoing hadron along the polarized nucleon's momentum direction in the e+N center-of-mass frame.

V. CONCLUSION

The observed π^+ and π^- asymmetries from ^3He and effective neutron targets have opposite signs when the target is transversely polarized. The π^+ and π^- asymmetries for a vertically polarized target are consistent with zero within the experimental uncertainties. Although the uncertainty is large, the sign of the $K^\pm A_{LT}$ is flipped as the target spin direction is reversed transversely (in the x-direction). The K^+ asymmetry is larger than that of π^+ and they are different in sign. If the kaon asymmetry is of partonic origin, it might indicate that sea-quark contributions or unfavored fragmentation functions play a more important role. In addition, higher-order or higher-twist effects might also be possible reasons. For the proton A_{LT} , the sign of the asymmetry is flipped as the target spin direction is reversed vertically (in the y-direction), while the asymmetry is consistent with zero within the experimental uncertainty with the target polarized transversely (in the x-direction). A hypothesis testing was performed to the proton asymmetries, the $\cos(\phi_s)$ dependence of the asymmetry can't be excluded within 2-sigma of significance. One of possible reasons for the interesting behavior of the proton asymmetries might be that the protons were mostly knocked out from ^3He with nuclear effects. In the collinear factorization approximation, A_{LT} in inclusive pion production was estimated in the JLab 6 GeV kinematic region [5]. The estimations were done using two approximations to calculate the $\tilde{g}(x)$ while doing numerical predictions for A_{LT} in inclusive pion production. One is using the approximate relation, $\tilde{g}(x) \approx -f_{1T}^\perp(x)$, where $f_{1T}^\perp(x)$ is the Sivers function; the other one is using Wandzura-Wilczek(WW)-type approximation, $\tilde{g}(x) \approx x \int_x^1 \frac{dy}{y} g_1(y)$. Calculations based on the two approximations shown in Figure 5 give different predictions. Our data are consistent in sign with the prediction using the WW approximation, while the magnitude of the predictions is larger than that of our

data. The calculation by using the Sivers function is not consistent with our data. However, one needs to take into account the current uncertainty of the Sivers function and potential large NLO corrections, which are not included in the calculation. We point out that p_T in our experiment is around 0.64 GeV/c, which is lower than 1 GeV/c where the theoretical predictions are believed to be reliable. In addition, the A_{LT} measurements in inclusive hadron production and SIDIS processes are linked by the definition of $\tilde{g}(x)$. The behavior of the π^+ and π^- $A_{LT}^{\cos(\phi_s)}$ with opposite sign is similar to that in the SIDIS measurement in [2], while the size of the asymmetries in inclusive and SIDIS processes are different. However, one has to be aware that the kinematic coverage for the non-detected electrons in the inclusive hadron production processes is larger than that of the electrons in the SIDIS processes and the production mechanism can also be different. To fully interpret the data, one has to understand the mechanism of inclusive hadron production in different kinematic regions and the main contributions to the double-spin asymmetry.

In summary, we have reported the measurement of A_{LT} in the inclusive hadron production reaction using longitudinally polarized electrons scattered from a transversely polarized ^3He target. Non-zero asymmetries were observed for charged pions from a transversely polarized

target. The asymmetries in π^+ and π^- production have opposite signs. The asymmetries are compared to calculations from collinear factorization, and the signs of the asymmetries are consistent with calculations using the WW approximation. To fully understand inclusive hadron production in terms of parton distributions and correlations among partons, new theoretical and experimental efforts should be carried out. Future experiments at Jefferson Lab [21, 22] and a future electron-ion collider (EIC) [23] will extend the measurement to a broad p_T range and a much higher precision.

VI. ACKNOWLEDGEMENTS

We acknowledge the outstanding support of the JLab Hall A staff and the Accelerator Division in accomplishing this experiment. This work was supported in part by the U. S. National Science Foundation, and by Department of Energy (DOE) contract number DE-AC05-06OR23177, under which the Jefferson Science Associates operates the Thomas Jefferson National Accelerator Facility. This work was also supported by the National Natural Science Foundation of China under Grants No. 11135002 and No. 11120101004 and the UK Science and Technology Facilities Council under Grants No. 57071/1 and No. 50727/1.

-
- [1] S. Kuhn, J.-P. Chen, and E. Leader, *Prog. in Part. and Nucl. Phys.* **63**, 1 (2009).
 - [2] J. Huang *et al.*, *Phys. Rev. Lett.* **108**, 052001 (2012).
 - [3] A. Afanasev, C. E. Carlson, and C. Wahlquist, *Phys. Rev. D* **58**, 054007 (1998).
 - [4] A. Afanasev, C. E. Carlson, and C. Wahlquist, *Phys. Rev. D* **61**, 034014 (2000).
 - [5] K. Kanazawa *et al.*, arXiv:1411.6459 (2014).
 - [6] J. Zhou, F. Yuan, and Z.-T. Liang, *Phys. Rev. D* **81**, 054008 (2010).
 - [7] Z.-B. Kang *et al.*, *Phys. Rev. D* **84**, 034046 (2011).
 - [8] A. Metz, D. Pitonyak, A. Schäfer, and J. Zhou, *Phys. Rev. D* **86**, 114020 (2012).
 - [9] J. Alcorn *et al.*, *Nucl. Instrum. Meth. A* **522**, 294 (2004).
 - [10] X. Qian *et al.*, *Phys. Rev. Lett.* **107**, 072003 (2011).
 - [11] K. Allada, Y. X. Zhao, *et al.* (Jefferson Lab Hall A Collaboration), *Phys. Rev. C* **89**, 042201 (2014).
 - [12] Y. X. Zhao *et al.* (Jefferson Lab Hall A Collaboration), *Phys. Rev. C* **90**, 055201 (2014).
 - [13] C. K. Sinclair *et al.*, *Phys. Rev. ST Accel. Beams* **10**, 023501 (2007).
 - [14] D. Androi *et al.*, *Nucl. Instrum. Meth. A* **646**, 59 (2011).
 - [15] F. Bissey, V. Guzey, M. Strikman, and A. Thomas, *Phys. Rev. C* **65**, 064317 (2002).
 - [16] E. Babcock, I. A. Nelson, S. Kadlecik, and T. G. Walker, *Phys. Rev. A* **71**, 013414 (2005).
 - [17] J. Singh *et al.*, arXiv:1309.4004 (2013).
 - [18] M. V. Romalis and G. D. Cates, *Phys. Rev. A* **58**, 3004 (1998).
 - [19] Y. Wang, Ph.D. thesis, UIUC (2011).
 - [20] S. Scopetta, *Phys. Rev. D* **75**, 054005 (2007).
 - [21] H. Gao *et al.*, *Eur. Phys. J.* **126**, 1 (2011).
 - [22] J.-P. Chen *et al.*, arXiv:1409.7741 (2014).
 - [23] A. Accardi *et al.*, arXiv:1212.1701 (2014).

	$\phi_s = 90^\circ$	$\phi_s = 270^\circ$
π^+	$0.0001 \pm 0.0015 \pm 0.0008$	$0.0006 \pm 0.0015 \pm 0.0008$
π^-	$-0.0007 \pm 0.0011 \pm 0.0008$	$-0.0004 \pm 0.0011 \pm 0.0008$
K^+	$0.007 \pm 0.023 \pm 0.003$	$0.017 \pm 0.024 \pm 0.004$
K^-	$0.011 \pm 0.032 \pm 0.005$	$0.044 \pm 0.033 \pm 0.006$
P	$0.0073 \pm 0.0047 \pm 0.0009$	$-0.0083 \pm 0.0047 \pm 0.001$
	$\phi_s = 0^\circ$	$\phi_s = 180^\circ$
π^+	$-0.0058 \pm 0.0016 \pm 0.0009$	$0.0071 \pm 0.0016 \pm 0.0009$
π^-	$0.0044 \pm 0.0011 \pm 0.0008$	$-0.0056 \pm 0.0011 \pm 0.0009$
K^+	$0.055 \pm 0.030 \pm 0.006$	$-0.066 \pm 0.031 \pm 0.006$
K^-	$0.014 \pm 0.040 \pm 0.006$	$-0.045 \pm 0.041 \pm 0.007$
P	$0.0032 \pm 0.0067 \pm 0.0008$	$-0.0013 \pm 0.0069 \pm 0.0008$

TABLE III. The beam-target double-spin asymmetries A_{LT} from ^3He for different hadron species. The data structure follows the format of asymmetry \pm statistical uncertainty \pm systematic uncertainty. The average p_T is 0.64 GeV/c.